Revision 1

Synthesis of Stoichiometric Nickel Aluminate Spinel Nanoparticles

Md. Hasan, John Drazin, Sanchita Dey, Ricardo H. R. Castro*

Department of Chemical Engineering and Materials Science, University of California - Davis, One Shields Avenue, Davis, CA 95616

*Corresponding author: rhrcastro@ucdavis.edu

Abstract

Nickel aluminate is a transition metal oxide with spinel structure with potential applications as catalysts and sensors. Both applications benefit from high specific surface areas as well as chemical stoichiometry control. However, a systematic approach to understand synthetic parameters affecting stoichiometry and agglomeration of nickel aluminate nanoparticles still lacks. In this work, co-precipitation using direct and reverse strikes and polymeric precursor techniques were comparatively studied to address this problem. While the polymeric method could deliver stoichiometric spinel, the samples were highly agglomerated exhibiting low surface area. Both co-precipitation procedures produced smaller sizes and less agglomerated nanoparticles as compared to the polymeric precursor, but for the reverse-strike, Ni^{2+} preferentially formed a soluble complex with ammonia and led to nickel deficient nanoparticles. Stoichiometric (1 mole NiO : 1 mole Al_2O_3) nanocrystalline nickel aluminate was only achieved when using controlled excess Ni^{2+}. The normal-strike lead to more stoichiometric compositions without need for excess cations, but the obtained nanoparticles were less homogeneous and showed smaller surface areas as compared to the reverse-strike method.

Keywords: Spinel, nickel aluminate, nanopowder, stoichiometry

Introduction

Aluminate spinels generally present high thermal stability and melting points, mechanical stability, and resistance to alkalis and acids (Zawadzki and Wrzyszcz, 2000). In particular, due to its defect chemistry, nickel aluminate is being considered in catalytic applications and proposed as a candidate material in high temperature fuel cells (Kou and Selman, 2000). $NiAl_2O_4$ is also a potential candidate in metal-ceramic composite because of its excellent strength and wettability with metal (Kim et al., 2000). In these applications, nano-sized particles are preferable as they can provide higher surface areas. Moreover, highly stoichiometric compositions are also of interest for those applications as are associated with higher melting points as compared to non-stoichiometric ones. Stoichiometry has also been shown to be of important for studies of relative stabilities of cations in octahedral and tetrahedral sites (Cooley and Reed, 1972); and studies of applications in radiation environments, given that stoichiometric spinels are more resistance to radiation damage than non-stoichiometric ones (Sickafus et al., 1996).

Several synthesis methods have been reported to obtain crystalline $NiAl_2O_4$ spinel with nano-sized particles (Cesteros et al., 2000; Clause et al., 1992; Deraz, 2013; Kiminami et al., 2005; Mohammadpour Amini and Torkian, 2002; Nazemi et al., 2012; Nogueira et al., 2007; Platero et al., 1999; Suciu et al., 2006). Among them, sol-gel method, using alkoxides as the precursor, was able to produce nanoparticle with particularly high surface area (Platero et al., 1999). But the cost of alkoxides and the byproducts of this method limit its engineering applications (Jeevanandam et al., 2002). Pechini method (Pechini, 1967), also known as modified sol-gel method, or polymeric precursor method (Cushing et al., 2004), was also successfully used to obtain highly homogeneous nickel aluminate spinel with small crystallite sizes (Kiminami et al., 2005; Segal, 1997). However, it has been recently reported that Pechini

method may leave serious carbonate contaminations during synthesis of spinels (Rufner et al., 2013). The contamination is typically located on the surface of the nanoparticles, which can lead to non-stoichimetric spinel structures because the carbonate phase may present a different cationic composition as the oxide. Coprecipitation method using direct strike has been reported to show advantages over the Pechini method in the preparation of $MgAl_2O_4$ in respect of purity, particle size distribution and agglomeration. This technique has also been studied to synthesize nickel aluminate spinel (Cesteros et al., 2000; Mohammadpour Amini and Torkian, 2002), but while particle size and surface area were reported previously, stoichiometry of the resultant spinel was not checked thoroughly in those studies, leaving a number of open questions, being the main one related to fact that nickel cations can easily form complexes in basic solution, possibly causing non-stoichimetric compounds upon co-precipitation.

In this work, we present an in-depth study of the stoichiometry, size and agglomeration states of nanoparticles prepared by three different methods: Pechini, reverse-strike co-precipitation and normal-strike co-precipitation. The goal is to identify the more adequate method to produce stoichiometric, size controlled and non-agglomerated particles by understanding and tuning the physical-chemistry of those methods.

Experimental Procedures

$NiAl_2O_4$ spinel Synthesis by Pechini Method

In the Pechini method, polyesterification is provoked in the presence of the cations, resulting in decorated resin since ions can form chelates with the non-reacted carboxyl groups from the polyester. The method then relies on the calcination of this resin and on the expectation that the nucleation of oxide particles upon calcination will take place at the same time as the

polymer degradation. This would allow nucleation sites to be sparse from each other while held by the three-dimensional rigid polymer structure. Ideally, once the polymer is fully degraded, the nanoparticles have all been nucleated. The method is very successful for the synthesis of single-metal oxides, but for double-metals, like aluminates, the process of spinel formation may take two steps. That is, it has been shown for $MgAl_2O_4$, for instance, an amorphous alumina structure is formed before formation of the aluminate, therefore, the final phase is only formed after the polymer is degraded, leading to agglomeration. Moreover, it has been shown that the combustion of the polymer can lead to increased temperatures, resulting in local high temperatures, also causing agglomerations (Rufner et al., 2013).

In this particular work, stoichiometric amounts of nickel nitrate [$Ni(NO_3)_2.6H_2O$. 98%] and aluminum nitrate [$Al(NO_3)_3 \cdot 9H_2O$, 98%] (Sigma Aldrich Inc., USA) were dissolved at in distilled water at room temperature. Citric acid [CA, $C_6H_8O_7$, 99%] and ethylene glycol [EG, $C_2H_6O_2$, 99.8%] (Sigma Aldrich Inc., USA) were then dissolved introduced to the ionic solution in amounts to reach the molar ratios of Ni^{2+}:Al^{3+}:CA:EG of 1:2:12:48. Polyesterification reaction is expected between CA and EG molecules due to the available carboxyl and hydroxyl groups. The proposed ratio assures though an excess of both reagents allowing branched polyesters and a diluted distribution of ions – allowing nucleation sites apart from each other. Polyesterification started when the solution was brought up to 120 °C on a stirring hot plate. Due to the use of nitrates as precursors, NO_x gas evolved during the process, resulting in a green viscous resin. The resin was brought to a furnace at 450 °C for 12 h under air to combust the resin and initiate nucleation. The product was crushed in a mortar and pestle and further calcined for different times under air. The post calcined powders had an intense blue coloration.

$NiAl_2O_4$ spinel Synthesis by Co-Precipitation Methods

Two variations of the co-precipitation method exist, differing basically on how the pH of the solution is changed to cause precipitation of the solubilized ions. In *reverse-strike co-precipitation*, a reaction bath with high pH, usually a base such as NH_4OH, is used and the cationic solution is added drop wise. This causes a precipitation shock: when the ionic solution gets in contact with the concentrated basic solution, a super-saturation condition is provoked for the formation of an hydroxide, allowing small sizes during nucleation (making use of traditional homogeneous nucleation theory (Cao, 2004)). In *normal-strike co-precipitation*, the base is added drop wise into the cationic solution to provoke precipitation of the hydroxide instead. Therefore, reverse-strike procedure is suggested to obtain higher cationic homogeneity in the precipitated hydroxide mixture, and smaller particle sizes (Vrolijk et al., 1990; Zhen et al., 2005).

However, co-precipitation procedures (either one) are not always chemically straight forward, specifically when dealing with synthesis of transition metal containing systems. In the presence of free NH_3, a soluble and stable (at high pHs) complex of the metal ion with NH_3 can be formed and, as a consequence, a portion of the transition metal ion is not precipitated. The resultant compound of course will deviate from stoichiometry, and adjustments are required to assure for compensation if highly stoichiometric materials are of interest.

In our experiments of co-precipitation, nickel nitrate [$Ni(NO_3)_2.6H_2O$. 98%] and aluminum nitrate [$Al(NO_3)_3 \cdot 9H_2O$, 98%] (Sigma Aldrich Inc., USA) were dissolved in deionized water with the help of magnetic stirrer. 1M aqueous ammonia solution was prepared from 25% ammonium hydroxide solution (Fisher Scientific, Inc.) to act as the precipitating agent. In the reverse-strike method, the cation solution was dripped into the 1M NH_4OH solution that was kept under vigorous stirring to assure homogenization of the solution once precipitation takes place, avoiding local pH fluctuations. An excess of NH_4OH solution was used to guarantee

no significant fluctuation of pH throughout the whole process. As soon as the salt solution was added to the precipitation solution, a greenish precipitate was observed throughout the mixed solution and the color of the supernatant turned blue. The precipitate (metal hydroxide) was then separated from the supernatant using centrifuge operated at 3000 rpm. The obtained powder was washed using deionized water and ethanol followed by centrifugation under similar conditions. The precipitate was dried over-night at 100 °C. The dried precipitate was ground using mortar and pestle and calcined at 800-1100°C for 12 h. As some Ni ions were lost by forming complex, to compensate this loss the Al-nitrate to Ni-nitrate molar ratios in the starting precursor was increased and several experiments were performed using different ratios, that is Ni:Al ratios of 2:2, 1.75:2, 1.625:2, 1.58:2, 1.55:2, 1.54:2, 1.50:2. 1.375:2, 1.25:2, 1:2.

In the normal-strike co-precipitation, 1M NH_4OH solution was added drop wise into the cationic solution. The initially green solution gradually turned into a turbid solution with white supernatant and greenish precipitates. In this case, exact amount of NH_3 solution was used to avoid the presence of excess of unreacted NH_3 that could complex with nickel ions and affect final stoichiometry of the precipitates. No significant amount of complex was formed as suggested by the color of the supernatant after the centrifugation.

Characterization of Nanoparticles

To find out the crystallization temperature of $NiAl_2O_4$, the co-precipitated hydroxide mixtures (and the Pechini resin) were heated at 10 °C/min to 1300 °C in a 100 μL platinum crucible under synthetic dry air flow of 20 ml/min using a Setaram SETSYS Evolution Differential Scanning Calorimeter and Thermal Gravimetric Analyzer (DSC/TGA) (Setaram

Instrumentation, Caluire, France). Powder X-ray diffraction patterns were obtained using a Bruker AXS D8 Advance powder diffractometer (Bruker AXS, Madi-son, WI) (Cu $K\alpha$ radiation, λ=1.5406 Å) operated at 40 kV and 40 mA. JADE 6.1 (MDI) software was used to perform a whole pattern profile fitting to determine crystal structure, phase purity, and crystallite size. Nitrogen absorption-desorption was performed using a Micromeritics ASAP 2020 analyzer (Micromeritics Instrument Corporation, Norcross, GA) equipped with a furnace and turbo pumps for degassing. Specific surface area was calculated using BET method.

Electron micro-probe analyzer (Cameca SX-100 Electron Microprobe) was used on sintered pellet to determine the chemical composition of the synthesized powders. At least ten random spots on the sample surface were chosen to check the homogeneity of composition. Sintering was done at 1350 °C for 4 h and before sintering, thermo gravimetric analysis of the powders were done up to 1400 °C to ensure that at the sintering temperature there would be no mass loss due to evaporation or reduction of the sample.

Particle size distributions and particle morphologies were determined through transmission electron microscopy (TEM) using a JEOL JEM-2500SE transmission electron microscope (Jeol Ltd., Tokyo, Japan) operated at 200 kV. Diffraction patterns were also taken using TEM.

Results

Reverse-strike Co-precipitation

The adopted co-precipitation procedure results in an amorphous hydroxide powder that should be further calcined to allow the transformation to crystalline oxides. As it is of interest to maintain small particle sizes, it is important to determine the lowest temperature at which the

158 oxide is being crystalized. Figure 1 shows the DSC/TGA performed on the as-precipitated
159 hydroxide for the composition Ni:Al equal 1:2. The thermogravimetry curve shows a decrease in
160 mass during the heating procedure, with basically two distinct slopes followed by leveling above
161 800 °C. While the weight loss below 200 °C can be attributed to physisorbed water, the one in
162 between 200 and 400 °C is most likely related to the transformation into oxide, resulting in H_2O
163 released as a product. The DSC signal shows a more complex profile, what can be attributed to
164 the small competitive processes taking place during calcination. That is, while generally water
165 desorption and transformation to oxide are the main phenomena expected, but the fact this is a
166 bi-cation system may allow multiple crystallization, and more information is needed to interpret
167 the curve.

168 Figure 2 shows the XRD from reverse-strike co-precipitation powder with 1:2 Ni:Al ratio
169 calcined at 450 °C. From the DSC/TG curves, this temperature is supposedly after most reactions
170 take place. However, the pattern reveals no presence of a spinel yet, with only nickel oxide
171 (NiO) crystalline phase observed, with a broad band attributed to an amorphous behind. This
172 indicates that amorphous aluminum hydroxide persists at this temperature and is consistent with
173 results for magnesium aluminates synthesis using similar technique (Rufner et al., 2013), where
174 the MgO phase is formed before the spinel. The results suggests that the small bump observed
175 from 400 °C to 650°C at the DSC/TG curve is most likely related to the dissolution of NiO
176 inside the amorphous hydroxide and concomitant formation of the new spinel phase. Another
177 exothermic heat is observed from 800 to 1200 °C, which is possibly due to coarsening of the
178 sample. To confirm both attributions, the sample was calcined at 1100 °C and characterized by
179 using XRD. The spinel phase (with absence of NiO or hydroxides) is observed to be formed, as
180 shown in Figure 3. Note that with this method, the spinel phase was already observed at 800 °C

181 though (pattern not shown here), and only coarsening was detected by further calcining at 1100
182 °C.

183 It is important to note however that the XRD pattern for the sample with 1:2 Ni:Al
184 precursor ratio does not correspond to $NiAl_2O_4$, but to a structure more similar to gamma-
185 alumina instead. This suggests non-stoichiometric samples as a result of Ni^{2+} complexion with
186 ammonium during precipitation. To assure stoichiometric samples are achieved, nickel to
187 aluminum ratio was varied from 2:2 to 1:2 by using the appropriate nitrate amounts. After
188 precipitation, the samples were calcined at 1100 °C. This relatively high temperature of
189 calcination was chosen to avoid the presence of too broad peaks of the aluminate that could
190 potentially hide the two characteristic XRD reflections of NiO and make structural analysis more
191 accurate.

192 Figure 4 shows the XRD patterns for each of the tested compositions. While all samples
193 resulted in spinel structures, increasing nickel content resulted in a shift of the parameters (Table
194 1) towards the stoichiometric $NiAl_2O_4$ spinel structure [PDF#78-1601]. Within the range 1.54:2
195 to 1.55:2 of molar ratio, the pattern perfectly matches expected stoichiometric $NiAl_2O_4$ lattice
196 parameters. Ratios above 1.55:2 showed a NiO second phase as evident from the peaks located at
197 43.3° and 62.8° in the XRD patterns. To confirm the chemical composition, Table 2 shows the
198 electron microprobe results for the samples produced with 1.55:2. The results indicate highly
199 stoichiometric powders, with virtually the theoretical atomic ratio. 10 different points were
200 studied in the sample to confirm homogeneity as noted in the experimental section.

201 While the samples showed stoichiometric, the grain sizes measured from XRD patterns
202 revealed coarsened samples (~51nm) as a result of the high calcination temperature. If the peak
203 found in the DSC curve going from 800 to 1200 °C is indeed solely related to coarsening, sample

calcination at 800 °C would enable the formation of the aluminate but with more limited grain growth. Hydroxides with 1.55:2 were then calcined at 800, 900, 1000 and 1100 °C. The sample calcined at 800 °C already revealed the formation of the nickel aluminate, and further treatment allowed coarsening as evident from the peaks' sharpening. Table 3 shows the grain sizes determined from the XRD patterns, revealing grains as small as 5nm for the sample calcined at 800 °C and systematic grain size increase with temperature.

Normal-strike Co-precipitation

Normal-strike co-precipitation is expected to show significantly less Ni^{2+} loss due to complexation as no excess of ammonia is used in the process. Therefore, solely the 1:2 Ni:Al ration was used to manufacture nanoparticles. Figure 1 shows the DSC/TG of the obtained hydroxide precipitate. The curves show communalities with the reverse-strike samples, with the weight change being almost identical, while the DSC signal showed differences in the 250 to 400 °C range. Figure 2 shows the XRD pattern for a powder calcined at 450 °C. Similarly to the reverse-strike method, a nickel oxide phase exists with absence of the spinel crystal structure and the existence of a broad background band attributed to the amorphous aluminum hydroxide. The sample was then further calcined at 1100 °C, a temperature where all reactions have taken place according to the DSC curve. The XRD pattern for this sample is shown in Figure 3. Spinel phase with peaks positioned consistent with the stoichiometric $NiAl_2O_4$ is observed and confirmed in by electron microprobe data in Table 2. Microprobe showed 0.985:2 for Ni:Al ratio, which can be considered stoichiometric as within experimental deviation, but the small difference as compared to the reverse-strike method can be attributed still to a slight formation of Ni^{2+} complexes with ammonia. Similarly to the reverse-strike method, aluminate was already the only

present phase at about 800 °C, but calcination at 1100 °C was performed for better structural analysis. In order to study the grain size of samples prepared by normal-strike precipitation, the samples were calcined at different temperatures. The samples calcined at 800, 900, 1000 and 1100 °C showed consistently larger grain sizes as compared to the reverse-strike, though being close to each other when considering the error bars.

Polymeric Precursor Method (Pechini)

The polymeric precursor method uses a significantly different method to achieve nanoparticles as compared to co-precipitation procedures. The nucleation process takes place while a polyester structure is still present, allowing diffusion limited nucleation and growth. Figure 1 shows the DSC/TG for the carbon rich powder obtained after calcination of the resin attained as described in the experimental section. The curve shows a significant mass loss (>90%), confirming the high percentage of carbon based materials related to residues from the polymer. Highly exothermic signals are observed, consistent with combustion and crystallization of an oxide phase. Figure 2 shows the XRD pattern for the powder calcined at 450 °C. Similarly to the co-precipitation samples, only nickel oxide was observed, with an amorphous band attributed to aluminum hydroxide. Interestingly, the peaks are much sharper than those from the co-precipitation powders, suggesting a larger grain size, what can be attributed to the combustion reaction, which may lead to local high temperatures, allowing enhanced coarsening.

The powder was further calcined at 800, 900, 1000 and 1100 °C to compare grain sizes and structures with the co-precipitation powders. Figure 3 shows the XRD for the 1100 °C, evidencing the nickel aluminate spinel structure. Grain sizes from XRD patterns for the different

249 temperatures are compiled in Table 3. Note that the grains are significantly larger for this method
250 as compared to both co-precipitation procedures regardless of the calcination temperature. The
251 smallest achievable grain size of pure spinel being 11.4 nm at 900 °C. That is, while the co-
252 precipitated powders had a NiO free spinel at 800 °C, this sample still had traces of the phase,
253 requiring higher temperature for complete NiO elimination. Table 2 shows the electron
254 microprobe results for the sample calcined at 1100 °C, revealing though a very stoichiometric
255 sample, attributed to the inexistence of parasite reactions to enable loss of nickel ions along the
256 process.

257 **Discussion**

258 All three studied methods successfully produced nickel aluminate nanoparticles. In order
259 to produce stoichiometric particles, the reverse-strike co-precipitation method needed direct
260 intervention and adjustment of initial concentrations due to the complex formation of Ni^{2+} with
261 the required excess of ammonia. That is, ammonium hydroxide solution was used as a
262 precipitation agent. The excess ammonia needed to provoke the supersaturated condition acts as
263 a ligand for the transition metal ion, such that Ni^{2+} forms a complex which is soluble in basic
264 solution. A blue color in the solution confirmed the presence of Ni^{2+} in solution after co-
265 precipitation. Hence, extra nickel precursor was needed to allow precipitation of the
266 stoichiometric compound ($NiAl_2O_4$).

267 This was confirmed by the lattice parameter analysis and direct elemental microprobe
268 (Table 1). That is, the ideal lattice parameter for stoichiometric $NiAl_2O_4$ spinel should be around
269 8.05Å. For the sample containing low Ni^{2+} content, the lattice parameter shifts towards gamma
270 alumina (7.905 Å) (Han et al., 2004). For the high concentration of Ni^{2+}, Ni^{2+} occupies not only

the typical tetrahedral coordination sites but also vacant octahedral ones. Because Ni^{2+} is larger than Al^{3+} (in terms of ionic radius), lattice expansion is observed. The expansion is however limited because of the oxygen vacancy formation induced by charge compensation mechanisms that will shrink the lattice. Note that high temperatures can also cause Ni^{2+} to shift to octahedral coordination, but at the temperature of processing here, this is not expected to take place (Han et al., 2004). The lattice parameter only agreed well with the theoretical $NiAl_2O_4$ value when using excess Ni^{2+} during synthesis, as confirmed by the elemental microprobe analysis, proving that Ni^{2+} is indeed lost during the reverse co-precipitation procedure. Pechini and normal-strike co-precipitation directly allowed highly stoichiometric samples.

On the other hand, as evidenced in Table 3, the grain sizes from the reverse-strike method are consistently smaller as compared to the other methods. Interestingly, the Pechini sample did not result in pure phase aluminate at 800 °C, and the sample showed a small amount of NiO. This can be attributed to the microstructure of the Pechini powder, which is expected to show more agglomerated particles (limiting the NiO reaction with the amorphous matrix to form the aluminate). Table 3 shows the results of surface area for samples calcined at 900 °C and measured by gas adsorption (BET). This temperature was selected as it is the lowest temperature where only nickel aluminate is observed regardless of the method. Note that the reverse-strike method showed the largest surface area (99 m^2/g), while the normal-strike was 19 m^2/g smaller, and Pechini was 50 m^2/g smaller. While this is simply qualitatively consistent with the grain sizes trend, a more detailed comparison between surface areas and grain sizes of each of the samples can provide information on state of agglomeration. That is, if one assumes a spherical-equivalent model, one can calculate the total interfacial area from the grain sizes. If all particles were non-agglomerated or partially sintered, the calculated interfacial area must be equivalent to,

or close to the surface area determined by gas adsorption. Otherwise, one can argue that there are significant amount of solid-solid interfaces that can be estimated by the difference between surface areas and calculated interfacial areas. For all methods, the calculations suggest some degree of agglomeration. This is expected as the samples were prepared at 900 °C, a temperature high enough to activate sintering mechanisms. A rough calculation shows the smaller degree of agglomeration for the reverse-strike, while the largest for the Pechini method. As previously reported (Dearden et al., 2013), the relatively lower agglomeration achieved by co-precipitation method as compared to Pechini can be attributed to the burn off stage of polymer that gives rise to localized temperature and enhanced agglomeration of the particles still in the early stage.

Figure 5 shows a collection of TEM images for the samples prepared by reverse-strike and Pechini. It is notorious that the co-precipitated samples are less agglomerated: while the measured grain sizes are consistent with those from XRD pattern fitting, the images show significant less neck formation and particle sizes for the co-precipitated samples. Interestingly, both images also reveal that the nanoparticles are anisotropic. This is not expected when using the adopted methods, but can be explained by the kinetics of particle nucleation and growth. That is, in all three methods, during calcination there is a competition between the formation of the spinel, NiO, and aluminum hydroxide. Because the aluminum hydroxide is a very stable phase considering its enthalpy of formation, it does not readily decompose to form the spinel, and NiO is formed as a transitional phase instead. Because nickel oxide is formed before the spinel phase, and this is surrounded by the aluminum hydroxide phase given the chemical environment of the nucleation, the process of formation of the spinel nanoparticles is, in all three cases, a solid state reaction between these two compounds. This enables growth of more stable facets, creating

highly anisotropic shapes. The large and strong agglomerates observed in the Pechini samples are thus believed to be responsible for the late reaction of NiO for the formation of the aluminate.

Implications

Several papers have reported on the synthesis of nickel aluminate nanoparticles, but critical sample parameters, such as the state of agglomeration and stoichiometry, are not commonly addressed. In this work we have demonstrated that the synthetic methods can easily led to strongly agglomerated and non-stoichiometric sample. We have shown though that fairly non-agglomerated and with small grain sizes (~5nm, ~100 m^2/g) $NiAl_2O_4$ particles can be obtained by a reverse-strike co-precipitation method after calcination at 800 °C. However, the method needed adjustment of stoichiometry though due to the complexion of Ni^{2+} with excess ammonia needed in the process. For the other two tested methods, Pechini and normal-strike co-precipitation, we also observed small grain sizes (~9 nm and ~6 nm, respectively) for calcinations at the same temperatures and fairly stoichiometric samples. However, the Pechini sample showed strong agglomeration (low surface area ~50 m^2/g) and still a second phase of NiO for powders calcined at 800 °C, and the normal-strike co-precipitation showed smaller surface area (~80m^2/g) as compared to the reverse-strike procedure. The higher overall quality of the particles obtained from the reverse-strike method can be explained by the overall concept underlying the procedure, that provokes a supersaturation condition to enable small critical nucleation sizes.

The possibility of fabricating $NiAl_2O_4$ nanoparticles with controlled stoichiometry opens a great perspective not only for manufacturing of bulk ceramics for structural studies, given that nanoparticles have high driving force for densification, but also for production of surface

controlled nanoparticles for catalytic applications. For instance, it has been shown that non-stoichiometric nickel aluminate is active for steam reforming of methane (Alubaid and Wolf, 1988). The refined control of stoichiometry of the nickel aluminate nanoparticles described in our work enables an unprecedented possibility for optimization of nanoparticles for such application.

References

Alubaid, A. and Wolf, E. E.(1988) Steam reforming of methane on reduced non-stoichiometric nickel alumiante catalysts. Applied Catalysis, 40(1-2), 73-85.

Cao, G. (2004) Nanostructures and Nanomaterials: Synthesis, Properties, and Applications. 433 p. Imperial College Press, Danvers.

Cesteros, Y., Salagre, P., Medina, F., and Sueiras, J.E. (2000) Preparation and characterization of several high-area $NiAl_2O_4$ spinels. Study of their reducibility. Chemistry of Materials, 12(2), 331-335.

Clause, O., Rebours, B., Merlen, E., Trifiro, F., and Vaccari, A. (1992) Preparation and characterization of nickel-aluminum mixed oxides obtained by thermal decomposition of hydrotalcite-type precursors. Journal of Catalysis, 133(1), 231-246.

Cooley, R.F., and Reed, J.S. (1972) Equilibrium cation distribution in $NiAl_2O_4$, $CuAl_2O_4$, and $ZnAl_2O_4$ spinels. Journal of the American Ceramic Society, 55(8), 395-398.

Cushing, B.L., Kolesnichenko, V.L., and O'Connor, C.J. (2004) Recent advances in the liquid-phase syntheses of inorganic nanoparticles. Chemical Reviews, 104(9), 3893-3946.

359 Dearden, C., Zhu, M., Wang, B., and Castro, R.H.R. (2013) Synthesis, size reduction, and
360 delithiation of carbonate-free nanocrystalline lithium nickel oxide. Journal of Materials
361 Science, 48(4), 1740-1745.
362 Deraz, N. (2013) Synthesis and Characterization of Nano-Sized Nickel Aluminate Spinel
363 Crystals. International Journal of Electrochemical Science. 8, 5203-5212.
364 Han, Y.S., Li, J.B., Ning, X.S., Chi, B. (2004) Effect of preparation temperature on the lattice
365 parameter of nickel aluminate spinel. Journal of the American Ceramic Society. 87(7)
366 1347–1349.
367 Jeevanandam, P., Koltypin, Y., and Gedanken, A. (2002) Preparation of nanosized nickel
368 aluminate spinel by a sonochemical method. Materials Science and Engineering: B,
369 90(1), 125-132.
370 Kim, J. W. Shin, P.W., Lee, M.J., Lee, S.J. (2000) Effect of particle size on the strength of a
371 porous nickel aluminate fabricated by polymer solution route. Journal of Ceramic
372 Processing Research, 7(2), 117-121.
373 Kiminami, R.H.G.A., Lira, H.L., de Melo Costa, A.C.F., Gama, L., Ribeiro, M., and de Oliveira,
374 J. (2005) Preparation and characterization of $NiAl_2O_4$ powder by the Pechini and
375 combustion methods. Materials Science Forum, 498, p. 722-727. Trans Tech Publ.
376 Kou, L., and Selman, J. (2000) Electrical conductivity and chemical diffusivity of $NiAl_2O_4$ spinel
377 under internal reforming fuel cell conditions. Journal of applied electrochemistry, 30(12),
378 1433-1437.
379 Mohammadpour Amini, M., and Torkian, L. (2002) Preparation of nickel aluminate spinel by
380 microwave heating. Materials Letters, 57(3), 639-642.

Nazemi, M., Sheibani, S., Rashchi, F., Gonzalez-DelaCruz, V., and Caballero, A. (2012) Preparation of nanostructured nickel aluminate spinel powder from spent NiO/Al_2O_3 catalyst by mechano-chemical synthesis. Advanced Powder Technology, 23(6), 833-838.

Nogueira, N.A.S., da Silva, E.B., Jardim, P.M., and Sasaki, J.M. (2007) Synthesis and characterization of $NiAl_2O_4$ nanoparticles obtained through gelatin. Materials Letters, 61(25), 4743-4746.

Pechini, N. (1967) U. S. Patent, n. 3.330.697.

Platero, E.E., Arean, C.O., and Parra, J. (1999) Synthesis of high surface area $CoAl_2O_4$ and $NiAl_2O_4$ spinels by an alkoxide route. Research on chemical intermediates, 25(2), 187-194.

Rufner, J., Anderson, D., Benthem, K., and Castro, R.H. (2013) Synthesis and Sintering Behavior of Ultrafine (< 10 nm) Magnesium Aluminate Spinel Nanoparticles. Journal of the American Ceramic Society.

Segal, D. (1997) Chemical synthesis of ceramic materials. J. Mater. Chem., 7(8), 1297-1305.

Sickafus, K.E., Yu, N., and Nastasi, M. (1996) Radiation resistance of the oxide spinel: The role of stoichiometry on damage response. Nuclear Instruments and Methods in Physics Research Section B: Beam Interactions with Materials and Atoms, 116(1), 85-91.

Suciu, C., Patron, L., Mindru, I., and Carp, O. (2006) Nickel aluminate spinel by thermal decomposition of polynuclear malate complexes. Revue Roumaine de Chimie, 51(5), 385.

Vrolijk, J.W.G.A., Willems, J.W.M.M., and Metselaar, R. (1990) Coprecipitation of yttrium and aluminium hydroxide for preparation of yttrium aluminium garnet. Journal of the European Ceramic Society, 6(1), 47-51.

Zawadzki, M., and Wrzyszcz, J. (2000) Hydrothermal synthesis of nanoporous zinc aluminate with high surface area. Materials research bulletin, 35(1), 109-114.

Zhen, Q., Kale, G.M., Shi, G., Li, R., He, W., and Liu, J. (2005) Processing of dense nanocrystalline Bi_2O_3-Y_2O_3 solid electrolyte. Solid State Ionics, 176(37), 2727-2733.

410

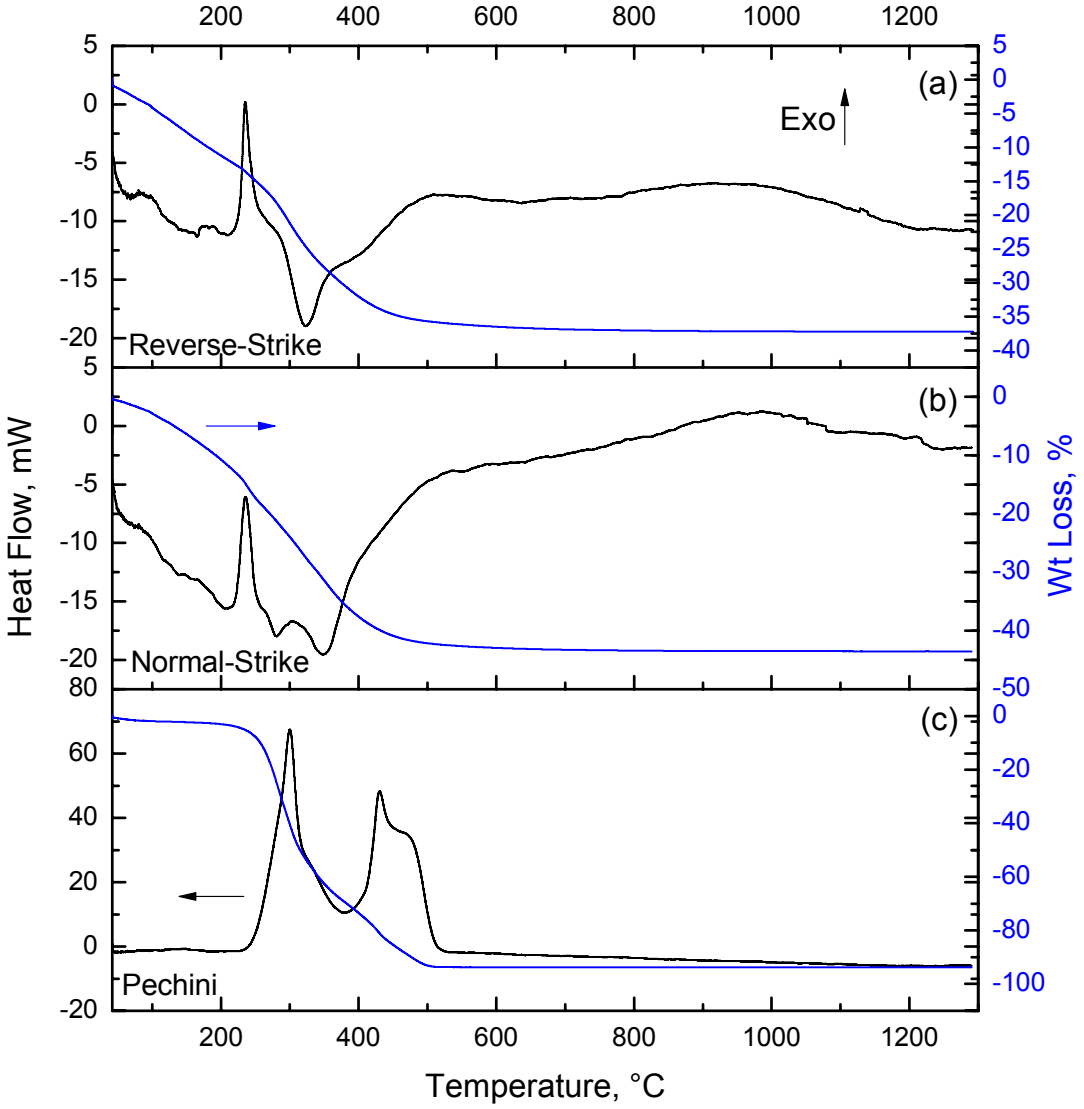

411

412 Figure 1. Differential scanning calorimetry (black line) and thermal gravimetric analysis (grey

413 line) of Pechini resin and co-precipitated hydroxides.

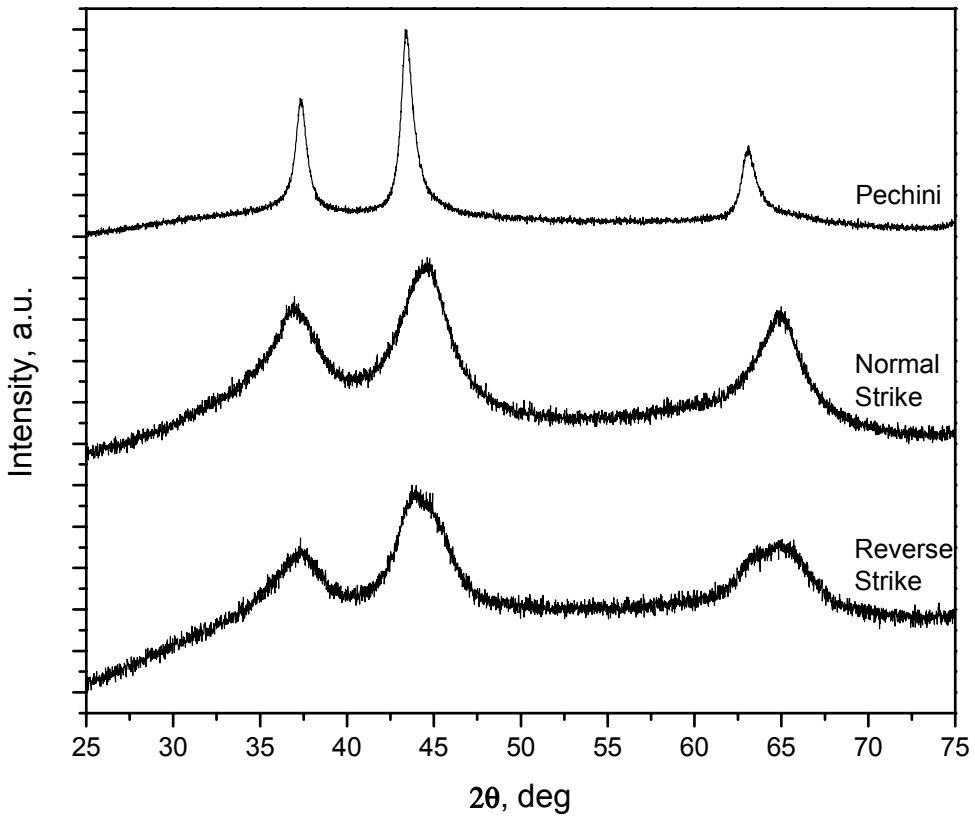

414

415 Figure 2. XRD patterns of the Pechini resin and co-precipitated hydroxides heat treated at 450 °C for

416 12 h showing the presence of NiO crystals

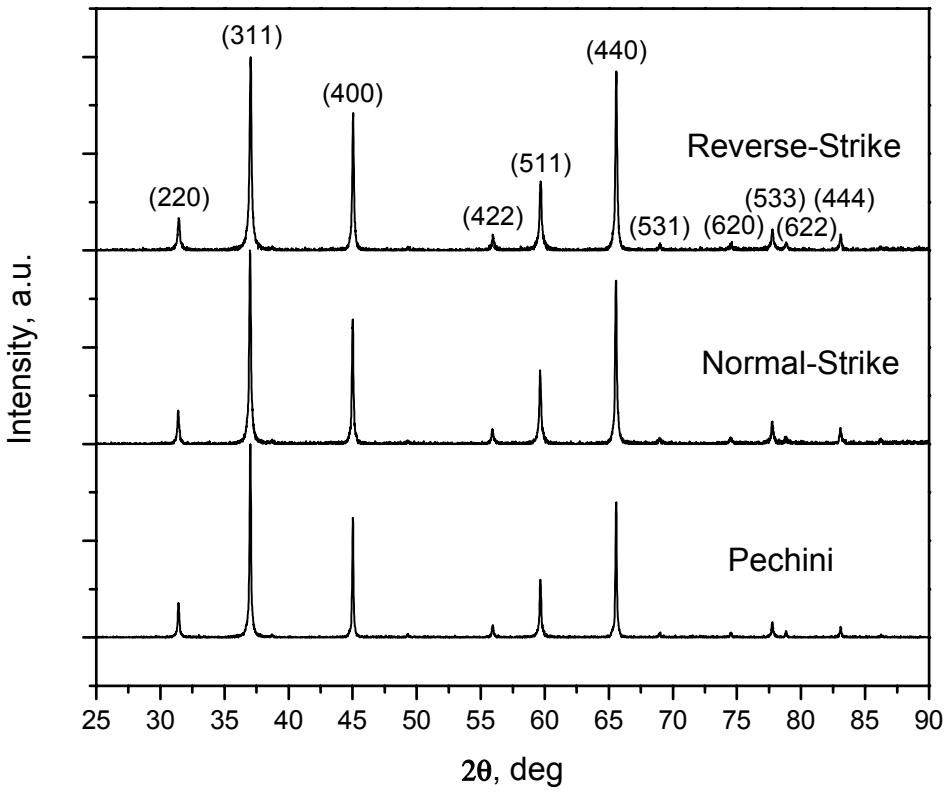

Figure 3. XRD data of nanoparticles synthesized by three methods and calcined at 1100 °C for 12 h.

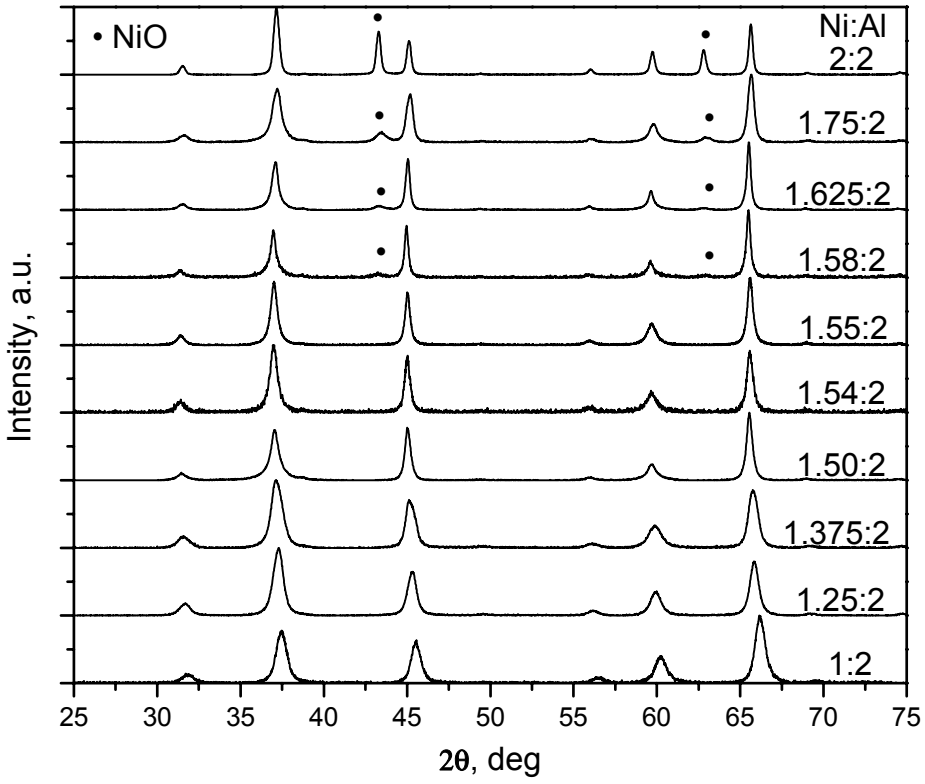

420

421 Figure 4. XRD patterns of the nanoparticles synthesized by reverse-strike co-precipitation with different

422 precursor molar ratios. Calcination was carried out at 1100°C for 2 hours.

423

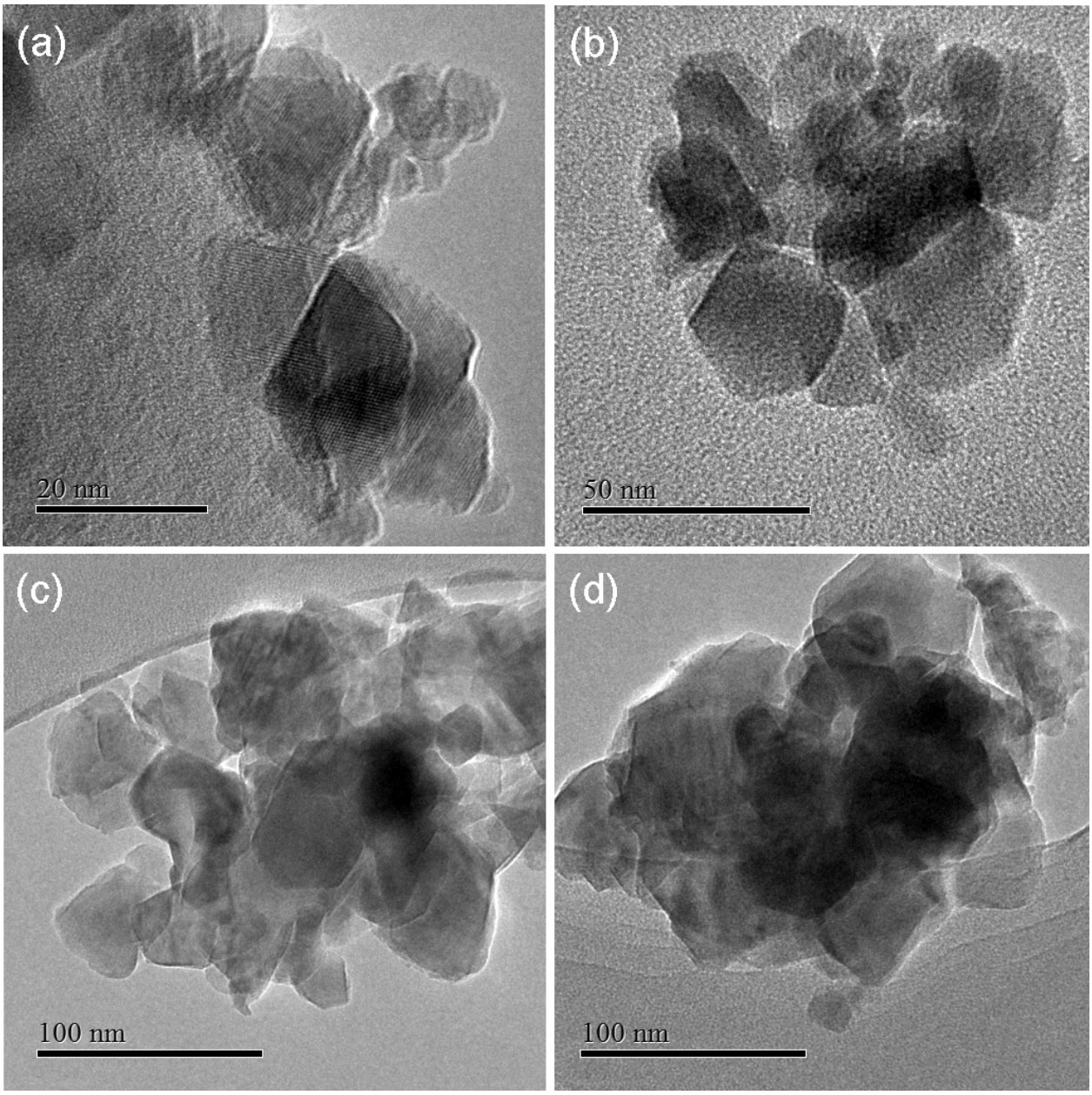

Figure 5. TEM micrographs of $NiAl_2O_4$ particles synthesized by reverse-strike co-precipitation (a and b) and Pechini method (c and d)

Tables

Table 1. Lattice parameters of the spinels synthesized by reverse-strike co-precipitation with different precursor ratios. Deviation in lattice parameters is smaller than 0.0005Å.

Ni:Al Precursor Ratio	Lattice Parameter(Å)
Ideal	8.0500
1:2	8.0045
1.55:2	8.0468
2:2	8.0560

435
436
437
438 Table 2. Microprobe results showing the stoichiometry of the spinels obtained by the three
439 methods.
440

	Stoichiometry		
	Al	**Ni**	**O**
Ideal	2	1	4
Pechini	2	1.0056±0.0258	4.0056±0.0258
Normal-Strike	2	0.9856±0.0196	3.9856±0.0196
Reverse-Strike	2	0.9997±0.0055	3.9997±0.0055

441
442

Table 3. Crystal Size and surface areas of powders synthesized by different methods. Surface area measurements have deviations of 0.5m^2/g.

	Reverse-Strike	**Normal-Strike**	**Pechini**
800 °C/12 h	4.9±0.8 nm	5.6±0.8 nm	8.9±1.3 nm (+NiO)
900 °C/12 h	8.3±1.1 nm	9.5±1.4 nm	11.4±1.4 nm
1000 °C/12 h	15.7±2.1 nm	19.7±2.4 nm	35.3±4.0 nm
1100 °C/12 h	51.5±4.9 nm	57.0±5.3 nm	73.3±5.1 nm
Surface area (m^2/g)	99 (900 °C)	80 (900 °C)	49 (900 °C)